

A novel label-free voltammetric immunosensor for the detection of α -fetoprotein using functional titanium dioxide nanoparticles

Wen-Bin Liang, Ruo Yuan*, Ya-Qin Chai, Yan Li, Ying Zhuo

Chongqing Key Laboratory of Analytical Chemistry, College of Chemistry and Chemical Engineering,
Southwest University, Chongqing 400715, China

Received 21 June 2007; received in revised form 21 September 2007; accepted 24 September 2007
Available online 7 October 2007

Abstract

A highly sensitive label-free voltammetric immunosensor was developed based on the functional titanium dioxide nanoparticles (PV–NTiP), which was prepared by capping 1,1'-bis-(2-phosphonoethyl)-4,4'-bipyridinium dibromide (PV) on the surface of the titanium dioxide nanoparticles (NTiP) with covalent attachment. The PV–NTiP has prominent biocompatibility, good electron transfer ability, primarily excellent adsorption, large specific surface area and positively charged environment. As a result, the negatively charged gold nanoparticles (NGP) could be adsorbed on the PV–NTiP modified electrode surface by electrostatic adsorption, and then to immobilize α -1-fetoprotein antibody (anti-AFP) for the assay of α -1-fetoprotein (AFP). The fabricated procedures and electrochemical behaviors of the immunosensor were characterized by electrochemical impedance spectroscopy (EIS), scanning electron microscopy (SEM) and cyclic voltammetry (CV). The anti-AFP/NGP/PV–NTiP modified electrode was sensitive to AFP in linear relation between 1.25 and 200 ng/mL with the correlation coefficient of 0.9982, and the detection limit ($S/N=3$) is 0.6 ng/mL under the optimal conditions. In addition, the proposed immunosensor exhibits good sensitivity, selectivity, stability and long-term maintenance of bioactivity and it may be used to immobilize other biomolecules to develop biosensor for the detection of other antigens or biocompounds.

© 2007 Elsevier Ltd. All rights reserved.

Keywords: 1,1'-Bis-(2-phosphonoethyl)-4,4'-bipyridinium dibromide (PV); Functional; Titanium dioxide nanoparticle (NTiP); Gold nanoparticle (NGP); α -1-fetoprotein (AFP); Immunosensor

1. Introduction

As a well-known tumor marker, α -1-fetoprotein (AFP), an oncofetal glycoprotein, is widely used for the diagnosis of hepatocellular carcinoma (HCC) [1–2]. Although, the total AFP level is high in healthy babyhood serum normally, it has reported that HCC could be suspected if the total AFP level is more than 20 ng/mL in adult serum [3–6]. Conventional methods for determination of AFP including enzyme-linked immunosorbent assay (ELISA), immunoradiometric assay (IRMA) and single radial immunodiffusion have some limitations such as relying on the label of either antigen or antibody, radiation hazards, a long analysis time and expensive instruments and/or skillful operators [7]. Thus, electrochemical immunosensors are of great interest due to their simple pretreatment procedure, fast

analytical time, precise current measurement and miniaturizable instrumentation compared with conventional immunoassay techniques [8–10].

Therefore, many kinds of electrochemical immunosensors have been developed [11–16]. Especially, the advanced materials based on nanoparticles, i.e. gold nanoparticles (NGP) are currently one of the key research fields. NGP had been extensively studied in analytical chemistry for their attractive physico-chemical characteristics [17–19] and comparatively good biocompatibility [20–27]. The reasons may be that the high surface to volume ratio and corresponding high surface energy of NGP resulted in the strong interaction between proteins and gold colloids, which may allow the protein molecules to orientate in a more favorable fashion on NGP surface [20,28–30] and the NGP could offer an environment similar to nature in the same time [18,31]. As a result the NGP could be utilized as an intermedator to immobilize bio-molecules to efficiently retain its activity in the construction of biosensors [32]. Recently, our group had reported immunosensors based

* Corresponding author. Tel.: +86 23 68252277; fax: +86 23 68254000.
E-mail address: yuanruo@swu.edu.cn (R. Yuan).

on NGP and titanium dioxide nanoparticles (NTiP) modified electrode with good accuracy and long-term stability [33,34]. However, the response current and sensitivity of the resulted immunosensor are limited, as the NTiP film which was modified on the electrode surface has showed high-electrochemical impedance.

N,N'-Disubstituted-4,4'-bipyridinium ions (viologen) have attracted much attention due to their good electron transfer ability. They play an important role as electron relays in systems in which electron transfer is initiated by electrochemical processes. The enhanced electron transfer from the nanoparticles to the bonded viologen is easy to take place when the distance is short [35], which make them useful in the electrochemical field. Since viologens are water soluble, any chemical device containing them must be based on immobilized viologens. In recent years, there are some reports about that the viologen with phosphonate linkers could be capped onto the NTiP surface based on the covalent coordination bond between the NTiP and phosphonate linkers in order to enhance the electrochemical response due to the good electron transfer ability of viologen [36]. The phosphonate linkers could bind the viologen to the surface of the NTiP strongly [37]. Thus, we synthesized one kind of viologen with phosphonate linkers, 1,1'-bis-(2-phosphonoethyl)-4,4'-bipyridinium dibromide (PV) bonded onto the NTiP surface to form functional nanostructure NTiP (PV-NTiP). This PV-NTiP shows many desired properties, such as prominent biocompatibility, good electron transfer ability, primarily excellent adsorption, large specific surface area and positively charged environment. The excellent characters make them useful to adsorb negatively charged NGP and be used in the field of immunosensors.

In this work, a novel functional NTiP (PV-NTiP) was synthesized by capping PV onto the NTiP surface at first. Then the prepared PV-NTiP was coated on the surface of a gold electrode to form a positively charged nanostructured monolayer. Subsequently, the negatively charged NGP was adsorbed on the PV-NTiP modified electrode surface by electrostatic adsorption. It could form a layer with larger surface and good biocompatibility and suitability for immobilization of α -1-fetoprotein antibody (anti-AFP) to obtain anti-AFP/NGP/PV-NTiP immunosensor. Details of the preparation, characterization and possible application of the immunosensor are described in the Section 2 followed.

2. Experimental and methods

2.1. Apparatus

Cyclic voltammetry (CV) and electrochemical impedance spectroscopy (EIS) measurements were performed with a Model IM6ex (ZAHNER Elektrick Co., Germany). A three-electrode system was used to consist the electrochemical cell where the gold electrode or modified gold electrode was used as the working electrode, a saturated calomel electrode (SCE) and a platinum wire were used as the reference and the counter electrode, respectively. All the potentials were reported versus the SCE reference electrode. The modifying progress was char-

actered based on S4800 scanning electron microscopy (SEM) (HITACHI Co., Japan). The structure of the PV was confirmed by AV-300 NMR instrument (Bruker Co., Switzerland) at ambient temperature at 300 and 121 MHz, respectively, and the gold nanoparticle sizes were confirmed by transmission electron microscopy (TEM) (H600, Hitachi Instrument, Co., Japan).

2.2. Reagents and materials

Anti-AFP and AFP were purchased from Biocell Co. (Zhengzhou, China). The NTiP was obtained from Sigma Chemical (St. Louis, USA). 4,4'-Bipyridinium was bought from J&K Chemical Ltd. (Beijing, China). All other reagents were analytical grade and used as received. All aqueous solutions were prepared with double-distilled, deionized water.

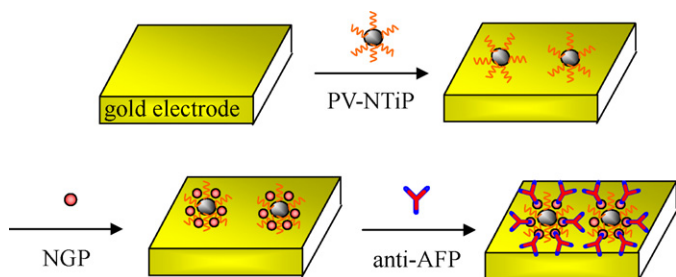
The NGP was prepared according to the literature [38] by adding 2 mL of 1% (w/w) sodium citrate solution into 50 mL of 0.01% (w/w) HAuCl₄ boiling solution. The particle sizes were confirmed by TEM, and the size of the prepared NGP is approximately 16 nm.

The PV was synthesized according to literature [39] by reaction of 4,4'-bipyridinium and bromine phosphonoethyl. The ester is hydrolyzed with aqueous HBr to obtain the diphosphonic acid and it was crystallized from isopropanol/water as brown solid. The structure of the PV was confirmed by ¹H NMR, ³¹P NMR. PV: ¹H NMR (D₂O, 300 MHz): δ (ppm) 2.45 (m, 4H), 4.90(m, 4H), 8.62 (d, $J=4.86$, 4H), 9.18(d, $J=4.86$, 4H); ³¹P NMR (D₂O 121 MHz): δ (ppm) 20.514.

The PV-NTiP was obtained as follow. Firstly, 1 mL NTiP solution was added into 1 mL 5 mmol/mL PV solution. And then, the mixed solution was stored at 4 °C for 12 h after being ultrasonicated for 30 min. The particle size of the PV-NTiP was characterized based on SEM and the SEM images were shown in Fig. 1.

2.3. Fabrication of the modified electrode

The modified gold electrodes (4 mm diameter) were prepared as follows. Prior to modification, the gold electrodes were polished carefully with the alumina slurries (0.3, 0.05 μ m). After the cleaning, the gold electrodes were ultrasonicated in acetone, water and ethanol two times, respectively. Next, polished gold electrodes were dipped in the 1:1 HCl:H₂O₂ mixture for 10–15 s, rinsed with a copious amount of water and dried in the air to remove the remained chemicals on the electrode surface. Following that, the PV-NTiP film were modified on the gold electrode surface by coating PV-NTiP on it and air-dried for 24 h. And then, the PV-NTiP modified electrodes were dipped in the NGP solution for 12 h to absorb NGP on the electrode surface. Subsequently, the NGP/PV-NTiP modified electrodes were immersed in the anti-AFP solution for 8 h at 4 °C. Finally, the anti-AFP modified electrodes were flushed in the BSA solution for 4 h at 4 °C in order to block possible remaining active sites of NGP monolayer and avoid the non-specific adsorption. The finished electrodes were stored at 4 °C when not in use. The schematic diagram



Scheme 1. The schematic diagram of the anti-AFP/NGP/PV-NTiP modified electrode procedures.

and the structure of the immunosensor procedures are shown in Scheme 1.

3. Results and discussion

3.1. The SEM images of the anti-AFP/NGP/PV/NTiP modified electrode

The SEM, which presents real particle shapes of the modified electrode surface, is able to provide a very useful data about the modifying progress. The SEM image of NTiP layer modified electrode was shown in Fig. 1A. In this image, we can see that the NTiP nanoparticles were distributed evenly with a mean size of 25 nm. As shown in Fig. 1B, the PV-NTiP particles were with a mean size of 30 nm, which is larger than that of the NTiP particles. It can be ascribed to that the PV had connected onto the surface of the NTiP particles. Fig. 1C is the image of the NGP

modified on the PV-NTiP membrane. It can be seen that the NGP with the mean size of 16 nm was successfully modified on the surface of the PV-NTiP membrane. Fig. 1D shows the image of anti-AFP/NGP/PV-NTiP with a changed structure of the particles, which indicates that the anti-body had been adsorbed on the surface of NGP successfully.

3.2. Electrochemical impedance characterization of the modifying process

EIS is a valuable and convenient tool to monitor the barrier of the modified electrode and an effective method to prove the interface properties of the surface-modified electrodes [40–42]. The complex impedance plots of different layer modified electrode were shown in Fig. 2. The complex can be presented as the sum of the real, $Z_{re} \Omega$ and imaginary, $Z_{im} \Omega$, components that originates mainly from the resistance and capacitance of the cell, respectively. The semicircle portion corresponds to the electron-transfer-limited that can be observed in the EIS. The semicircle diameter in the impedance spectrum equals to the electron-transfer resistance, R_{et} , which could be computed based on the model impedance data of redox couples accurately.

Here, the modified electrode was measured by EIS in the solution of 2 mmol/L $[\text{Fe}(\text{CN})_6]^{4-}/[\text{Fe}(\text{CN})_6]^{3-}$ (1:1) with 0.1 mol/L KCl at the frequency range from 5×10^{-2} to 1×10^6 Hz in a given open circuit voltage, amplitude was 10 mV, and the result was shown in Fig. 2. As shown in Fig. 2a, a very low interfacial R_{et} ($R_{et} = 26.86 \Omega$) can be found, which implied

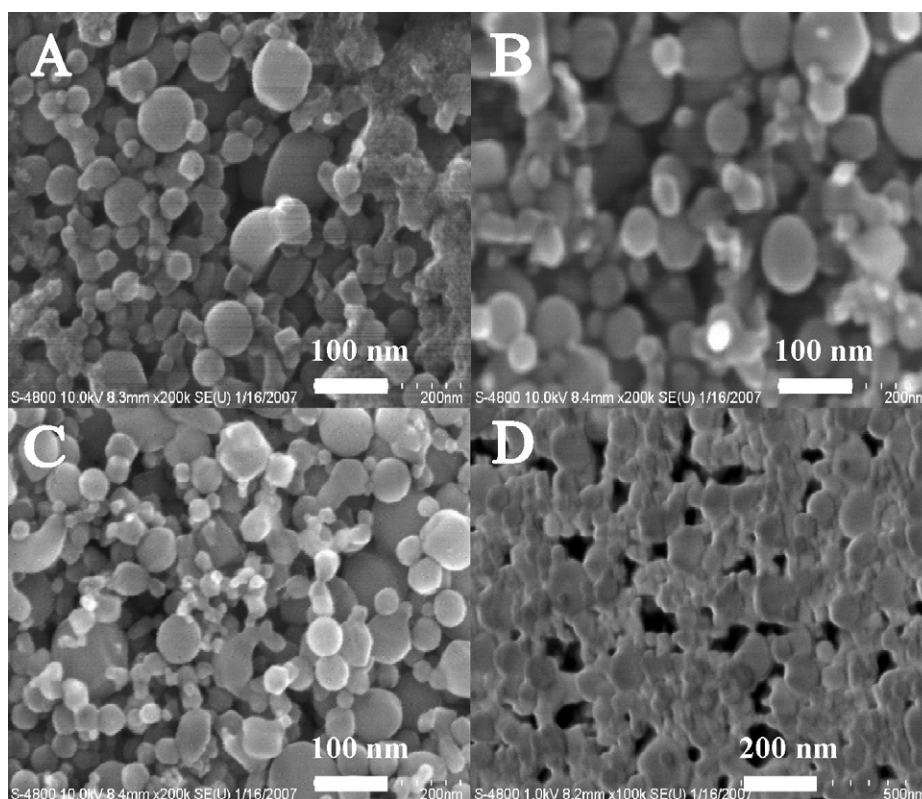


Fig. 1. The SEM images of the NTiP (A), PV-NTiP (B), NGP/PV-NTiP (C) and anti-AFP/NGP/PV-NTiP (D).

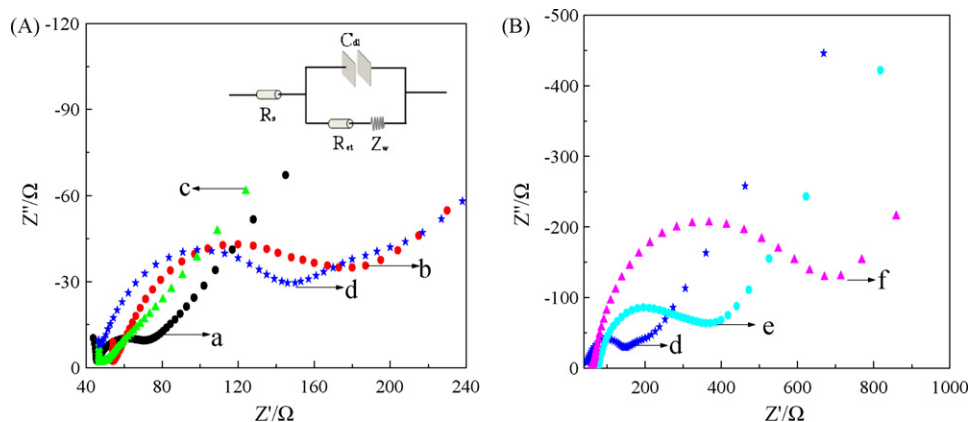


Fig. 2. The EIS of the bare and different modified electrodes. Fig. 4A is the EIS of the bare electrode (a) and electrodes modified of NTiP (b), PV-NTiP (c) and PV-NTiP/NGP (d); Fig. 4B is the EIS of the different modified electrodes after the modifying of NGP (d), anti-AFP (e) and BSA (f). Insert in (A): the equivalent circuit used to model impedance data in the presence of redox couples: R_s : electrolyte resistance; R_{et} : electron transfer resistance; Z_w : Warburg impedance; C_{dl} : double-layer capacitance.

that the characteristic of a diffuse limiting step of the electrochemical process on the bare gold electrode. After the modifying of PV-NTiP (Fig. 2b), the R_{et} decreased to 15.25Ω due to the good electron transfer ability of PV-NTiP. After the adsorption of negatively charged NGP onto the electrode surface, an increased interfacial R_{et} ($R_{et} = 114.35 \Omega$) was observed (Fig 2d). The R_{et} increased to 145.35Ω after the immobilization of anti-AFP, which is attributed to that the membrane of the protein insulates the conductive support and counteract the interfacial electron transfer. In addition, the EIS of PV-NTiP modified electrode compared with NTiP modified electrode was shown in inset of Fig. 2. In this figure, we can see that the R_{et} of PV-NTiP (15.25Ω) modified electrode decreased a lot than it of NTiP (111.97Ω) modified electrode as the PV-NTiP displays more excellent electron transfer ability. It could be considered as the NTiP layer with high resistance obstructed electron-transfer and the PV-NTiP layer's structure was changed after the PV was modified on NTiP nanoparticles surface by chemisorption. The electron-transfer fashion was changed and the scheme was shown in Fig. 3. In addition, the positively charged PV-NTiP surface also could reduce the impedance of the PV-NTiP modified layer.

3.3. Cyclic voltammetry characterization of the modifying process

Electroactivity of the modified electrodes were studied using CV to obtain information about reagent immobilization, activ-

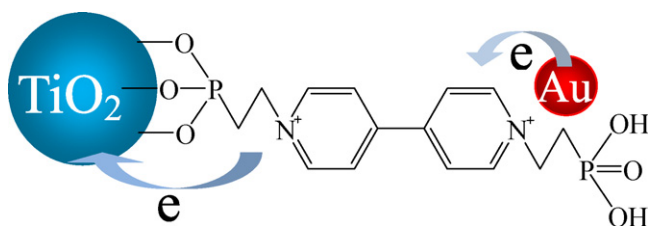


Fig. 3. The schematic map of electron transfer on the NGP/PV-NTiP layer.

ity, and stability, respectively. Fig. 4a displays the CV of bare electrode. When the PV-NTiP was modified, an increase of the current response can be found in Fig. 4b, which indicates the good electron transfer ability of the PV-NTiP. The formation of the NGP/PV-NTiP modified electrodes was shown in curve c. There is an obvious reduce of current response as the negatively charged NGP blocked the electron transfer based on the electrostatic interaction between NGP and negatively charged $[\text{Fe}(\text{CN})_6]^{4-}$. Curve 4d shows the CVs of the BSA/anti-AFP/NGP/PV-NTiP modified electrodes. The decreases of the current responses can be seen, which demonstrate the membrane became less conductive as the protein adsorbed. In addition, the CVs of PV-NTiP modified electrode compared with it of NTiP modified electrode were showed in Fig. 4 inset. It can be seen that the PV-NTiP modified electrode (Fig. 4b) shown a higher current response than that of NTiP modified electrode (Fig. 4e), since PV-NTiP exhibited good electrode transfer ability.

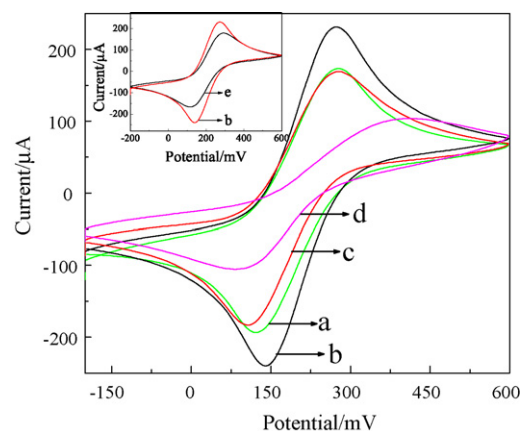


Fig. 4. CVs of the different electrodes (a) bare electrode, (b) PV-NTiP modified electrode, (c) NGP/PV-NTiP modified electrode, (d) BSA/anti-AFP/NGP/PV-NTiP modified electrode and (insert e) NTiP modified electrode at 100 mV/s scan rate in the solution of $2 \text{ mmol/L } [\text{Fe}(\text{CN})_6]^{4-}/[\text{Fe}(\text{CN})_6]^{3-}$ (1:1) with 0.1 mol/L KCl .

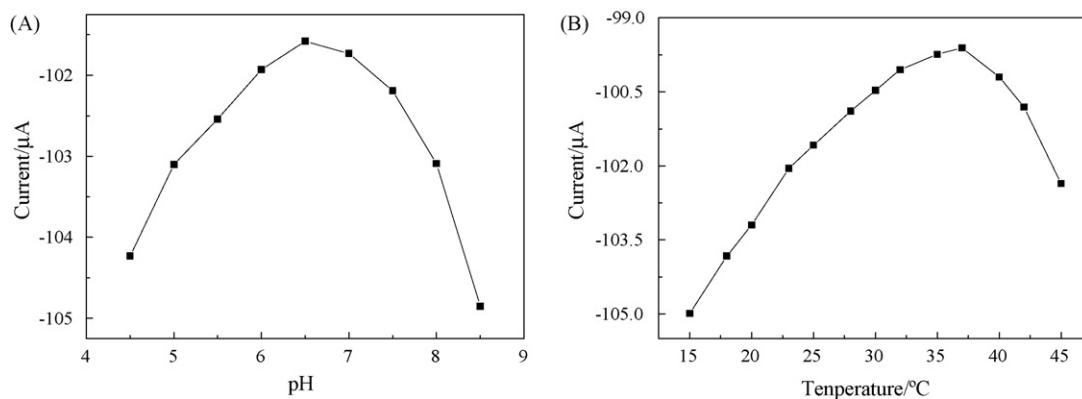


Fig. 5. The optimization condition for the immunosensor based on the pH (A) and temperature (B).

3.4. Optimization of the assay conditions

The effect of pH on the immunosensor response signals lies in two main aspects: one is the effect on the antigen and antibody, unsuitable pH may cause protein denaturalization; the other is the effect on the affinity between the active material, the protein and the electrode surface. Fig. 5A shows the effect of pH on the immunosensor in the pH range of 4.5–8.5. As shown in Fig. 5A, the current response reached the maximum at pH 6.5, and then the current response reduced if the pH higher or lower than pH 6.5. The reason may be that, the higher and lower pH may damage the protein and effect the lifetime of the immunosensor. Considering the response and the lifetime of the immunosensor, the pH 7.0 was used as a compromise.

The effect of the temperature is important on the activity of the antigen and antibody. The study of the temperature influence from 15 to 45 °C was shown in Fig. 5B. As shown in Fig. 5B, an increase temperature had a favorable effect on the immunoreaction and reached a maximum value at 37 °C. It is well known that an optimal temperature immunoreaction would be 37 °C. Considering the easy-to-use of the immunosensor, the 25 °C (normal room temperature) was recommended to be used as measure temperature in our study.

The immunochemical incubation time (when the antigen-antibody reaction occurs in the solution without stirring) is another influence condition of the immunosensor. When the analyte antigens reached the antibodies modified on the surface of the immunosensor, it would take some time for the contracting species to form immunocomplexes. The influence of the immunochemical incubation time of the immunosensor on the response signals was investigated. In the first 6 min, the response current was rapidly down and it reached an equilibration state when the immunochemical incubation time over 6 min. Thus, the immunochemical incubation time of 6 min was selected for all the subsequent assays.

3.5. The detection of the AFP based on CV

The calibration curve for AFP detection with anti-AFP/NGP/PV-NTiP-modified gold electrode was obtained in

a conventional electrochemical cell with a potential swept from -0.2 to 0.6 V (versus SCE) and a sweeping rate of 100 mV/s in 2 mmol/L $[\text{Fe}(\text{CN})_6]^{4-}/[\text{Fe}(\text{CN})_6]^{3-}$ (1:1) + 0.1 mol/L KCl after the immunosensor was incubated in 0.5 mL standard solution with different concentration at room temperature for 6 min without stirring the solution (Fig. 6). The current response values of the immunosensor are sigmoidal with the values of AFP concentration ranging from 0.25 to 300 ng/mL (Fig. 6). As expected, the response signal decreased with the increase of AFP concentration since AFP-anti-AFP immunocomplexes would increase the resistance of the immunosensor. The immunosensor showed a linear range between 1.25 and 200 ng/mL with a regression equation of the form I (μA) = -0.0795 [AFP] (ng/mL) + 0.0572 (I is the cathodic peak current) with the correlation coefficient of 0.9982 and the detection limit of 0.6 ng/mL at 3δ (where δ is the standard deviation of zero-dose response $n = 11$). Furthermore, the response time of the immunosensor is about 16 s.

In addition, we had studied two other different immunosensor as contrast: BSA/anti-AFP/NTiP and BSA/anti-AFP/NGP/NTiP. The result was showed in Table 1, which indicated that the PV-NTiP used in the field of voltammetric immunosensor could increase the sensitivity greatly.

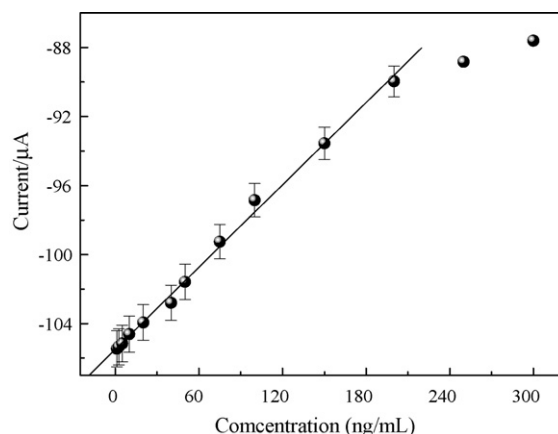


Fig. 6. The calibration plots for the immunosensor current responses of different concentration of AFP.

Table 1
The contrast results of different immunosensors

| Parameter | Immunosensors | | |
|-------------------------------|---------------|-------------------|----------------------|
| | Anti-AFP/NTiP | Anti-AFP/NGP/NTiP | Anti-AFP/NGP/PV–NTiP |
| Linear response range (ng/mL) | 2.5–180 | 2.0–200 | 1.25–200 |
| Sensitivity (ng/mL) | 0.0375 | 0.0413 | 0.0795 |
| R.S.D. (%) ^a | 4.26 | 3.13 | 2.41 |
| Low detection limit (ng/mL) | 1.3 | 0.9 | 0.6 |

^a The R.S.D. was obtained from 10 measurements by using 20 ng/mL as the model.

Table 2
Experimental results of different methods obtained in serum samples

| | Sample number | | | |
|--|---------------|--------------|--------------|--------------|
| | 1 | 2 | 3 | 4 |
| By developed method (ng/mL) ^a | 17.56 ± 0.06 | 23.43 ± 0.07 | 38.97 ± 0.13 | 58.51 ± 0.19 |
| By ELISA (ng/mL) | 16.00 ± 0.05 | 21.10 ± 0.06 | 37.32 ± 0.10 | 57.14 ± 0.16 |
| Relative error (%) | 109.8 ± 1.6 | 111.0 ± 0.4 | 104.4 ± 0.3 | 102.4 ± 0.4 |
| <i>F</i> value ^b | 1.34 | 1.21 | 1.38 | 1.33 |

^a The values were the mean values from 10 measurements.

^b There is no distinct difference between the developed method and ELISA, if the *F* value is smaller than $F_{(0.10, 9, 9)}$ (3.18).

3.6. Interference experiments of the modified electrodes

Interference experiments were performed to assess whether the immunosensors could respond selectively to different kinds of antigens. The immunosensor was used to detect two of 100 ng/mL AFP incubating solution: one solution with the interferent (CEA, glutamic acid, dopamine, vitamin C, benzedrine acid, IgG and BSA) and the other without. The results shown that the peak current responses in the two solutions showing less than 4.6% difference, which means that the immunosensor in this study could respond to AFP specifically.

3.7. Regeneration and reproducibility of the modified electrodes

Regeneration of the immunosensor is an important character. In our experiment, we studied some regenerative reagents (glycine, NaOH/HCl, HCl and urea). After completing each assay, the same immunosensor was immersed in one of the regenerative reagents solutions for about 5 min and removed to wash with water to dissociate the antigen–antibody complex. As a result, the glycine (pH 3.0) was the best one with the response error of the renewable of 2.5% (five regenerations and measurements). Successive experiments shown the biosensor based on the anti-AFP/NGP/PV–NTiP membrane could be regenerated by simple method.

3.8. Stability of the modified electrodes

The stability is one of the important characteristics of the biosensor. In this work, the stability of the modified electrode was measured based on the CVs examined in 2 mmol/L $[\text{Fe}(\text{CN})_6]^{4-}/[\text{Fe}(\text{CN})_6]^{3-}$ (1:1) + 0.1 mol/L KCl with a potential swept from –0.2 to 0.6 V (versus SCE) and a sweeping

rate of 100 mV/s. As expect, the calculated relative standard deviation (R.S.D.) of 2.1% was observed after 50 circles CV measurements. Moreover, long-term stability was investigated. Only 5.2% deterioration of peak currents was found during 60 days storage of the immunosensor. Thus, the immunosensor could be used for long-term measurements and have good stability and reproducibility. In addition, we used 20 ng/mL AFP as a model to examine the stability of the immunosensor and used test of significance to examine this method with systematic error or not. As expect, the confidence interval is 20.02 ± 0.06 ng/mL and the *t* value is 0.57, which is smaller than $t_{(0.05, 9)}$, so there is no systematic error in this method and could be used for the AFP analysis.

3.9. Application of the immunosensor

Furthermore, to demonstrate the use of the proposed immunosensor to be applied for clinical analysis, four human serum specimens from college students at our university hospital were examined by the studied immunoassay and the ELISA method. A part of the results are showed in Table 2. A good correlation was found between the results of the two methods and the *F* value obtained by test of significance is smaller than $F_{(0.10, 9, 9)}$, which suggest that there are no difference of significance between the two methods and the immunosensor could be used for the determination of AFP concentration in serum feasibly.

4. Conclusion

In this experiment, we describe a novel immobilization strategy based on PV–NTiP and NGP to immobilize anti-AFP on the surface of the gold electrode to construct a new immunosensor for the determination of AFP with a good sensitivity, selectivity,

stability and long-term maintenance of bioactivity. Although the strategy has been applied to use AFP as a model system only in this work, it could be extended toward other clinically or environmentally interested bio-species.

Acknowledgements

This work was supported by the National Natural Science Foundation of China (29705001), the Natural Science Foundation of Chongqing City, China (CSTC 2004BB4149, 2005BB4100) and High Technology Project Foundation of Southwest University (XSGX02).

References

- [1] E. Alpert, R. Hershberg, P.H. Schur, K.J. Lselbacher, *Gastroenterology* 61 (1971) 137.
- [2] K. Okuda, *Dig. Dis. Sci.* 31 (1986) 133.
- [3] K. Okuda, K. Kotoda, H. Obata, N. Hayashi, T. Hisamatsu, M. Tamiya, Y. Kubo, F. Yakushiji, E. Nagata, S. Jinnouchi, Y. Shimokawa, *Gastroenterology* 69 (1975) 226.
- [4] F. Nomura, K. Ohnishi, Y. Tanabe, *Cancer* 64 (1989) 1700.
- [5] H. Oka, A. Tamori, T. Kuroki, K. Kobayashi, S. Yamamoto, *Hepatology* 19 (1994) 61.
- [6] I. Stefanova, V. Horejisi, H. Kristofova, P. Angelisova, V. Zizkovsky, I. hilgert, *J. Immunol. Methods* 111 (1988) 67.
- [7] K. Sato, A. Hibara, M. Tokeshi, H. Hisamoto, T. Kitamori, *Adv. Drug. Deliv. Rev.* 55 (2003) 379.
- [8] H. Tsutsumi, K. Takeoka, T. Oishi, *J. Colloid Interface Sci.* 185 (1997) 432.
- [9] S. Storri, T. Santoni, M. Minunni, M. Mascini, *Biosens. Bioelectron.* 13 (1998) 347.
- [10] T. Hianik, M. Snejdarkova, L. Sokolikova, E. Meszar, R. Krivanek, V. Tvarozek, I. Novotny, J. Wang, *Sens. Actuators B* 57 (1999) 201.
- [11] Y. Zhuo, R. Yuan, Y.Q. Chai, D.T. Tang, Y. Zhang, N. Wang, X.L. Li, Q. Zhu, *Electrochem. Commun.* 7 (2005) 355.
- [12] Y. Zhuo, R. Yuan, Y.Q. Chai, Y. Zhang, X.L. Li, N. Wang, Q. Zhu, *Sens. Actuators B* 114 (2006) 631.
- [13] F. Darain, S.U. Park, Y.B. Shim, *Biosens. Bioelectron.* 18 (2003) 773.
- [14] Z. Dai, F. Yan, H. Yu, X.Y. Hu, H.X. Ju, *J. Immunol. Methods* 287 (2004) 13.
- [15] H. Yu, F. Yan, Z. Dai, H.X. Ju, *Anal. Biochem.* 331 (2004) 98.
- [16] J. Yakovleva, R. Davidsson, A. Lobanova, M. Bengtsson, S. Eremin, Y. Laurell, J. Emneus, *Anal. Chem.* 74 (2002) 4814.
- [17] L. Wang, E. Wang, *Electrochem. Commun.* 6 (2004) 225.
- [18] D.P. Tang, R. Yuan, Y.Q. Chai, X. Zhong, Y. Liu, J.Y. Dai, *Biochem. Eng. J.* 22 (2004) 43.
- [19] S.Y. Xu, X.Z. Han, *Biosens. Bioelectron.* 19 (2004) 1117.
- [20] H. Zhang, H.Y. Lu, N.F. Hu, *J. Phys. Chem. B* 110 (2006) 2171.
- [21] R. Elghanian, J.J. Storhoff, R.C. Mucic, R.L. Letsinger, C.A. Mirkin, *Science* 277 (1997) 1078.
- [22] J. Zhao, J.P. O'Daly, R.W. Henkens, J. Stonehuerner, A.L. Crumbliss, *Biosens. Bioelectron.* 11 (1996) 493.
- [23] S. Nie, S.R. Emory, *Science* 275 (1997) 1102.
- [24] L.A. Lyon, M.D. Musick, M.J. Natan, *Anal. Chem.* 70 (1998) 5177.
- [25] A. Doron, E. Katz, I. Willner, *Langmuir* 11 (1995) 1313.
- [26] K.R. Brown, A.P. Fox, M.J. Natan, *J. Am. Chem. Soc.* 118 (1996) 1154.
- [27] A.L. Crumbliss, S.C. Perine, J. Stonehuerner, K.R. Tubergen, J. Zhao, R.W. Henkens, J.P. O'Daly, *Biotechnol. Bioeng.* 40 (1992) 483.
- [28] S.Q. Liu, D. Leech, H.X. Ju, *Anal. Lett.* 36 (2003) 1.
- [29] C.X. Lei, S.Q. Hu, N. Gao, G.L. Shen, Yu S R.Q., *Bioelectrochemistry* 65 (2004) 33.
- [30] R. Shukla, V. Bansal, M. Chaudhary, A. Basu, R.R. Bhone, M. Sastry, *Langmuir* 21 (2005) 10644.
- [31] J. Wu, J.H. Tang, Z. Dai, F. Yan, H.X. Ju, N.E. Murr, *Biosensors and Bioelectronics* 22 (2006) 102.
- [32] C.X. Lei, F.C. Gong, G.L. Shen, R.Q. Yu, *Sens. Actuators B* 96 (2003) 582.
- [33] Y.T. Shi, R. Yuan, Y.Q. Chai, X.L. He, *Electrochim. Acta* 52 (2007) 3518.
- [34] Y.T. Shi, R. Yuan, Y.Q. Chai, M.Y. Tang, X.L. He, *J. Electroanal. Chem.* 604 (2007) 9.
- [35] H. Hosono, M. Kaneko, *J. Photochem. Photobiol. A* 107 (1997) 63.
- [36] A. Deronzier, J.C. Moutet, *Acc. Chem. Res.* 22 (1989) 249.
- [37] B. Long, K. Nikitin, D. Fitzmaurice, *J. Am. Chem. Soc.* 125 (2003) 5152.
- [38] L.A. Vermeulen, M.E. Thompson, *Lett. Nat.* 358 (1992) 656.
- [39] G. Frens, *Nat. Phys. Sci.* 241 (1973) 20.
- [40] E. Katz, I. Willner, *Electroanalysis* 15 (2003) 913.
- [41] V. Pardo-Yissar, E. Katz, J. Wasserman, I. Willner, *J. Am. Chem. Soc.* 125 (2003) 622.
- [42] A. Bardea, E. Katz, I. Willner, *Electroanalysis* 12 (2000) 1097.